



Development and Characterization of Anti-Perovskite Structured Nickel-Iron Nitride Electrocatalyst for Oxygen Evolution Reaction

Doğaç Turan¹  and M. Kadri Aydınol² 

¹ Middle East Technical University, Ankara 06800, Turkey

² Middle East Technical University, Ankara 06800, Turkey
dogac.turan@metu.edu.tr

Abstract. Electrochemical water splitting is a key method for clean, sustainable, and green hydrogen production, in which hydrogen evolution reaction (HER) and oxygen evolution reaction (OER) are the essential reactions underlying this phenomenon. These reactions are relatively sluggish in the perspective of reaction kinetics, which need to be catalyzed by electrocatalysts, like Pt/C, IrO₂, and RuO₂. However, these are problematic electrocatalysts when large-scale applications are considered in terms of affordability and scarcity of the precious elements. In this study, we aim to develop more accessible and affordable electrocatalysts containing relatively abundant elements used in alkaline conditions. Accordingly, the electrocatalytic properties of the anti-perovskite structure Ni₃FeN compound were investigated. Single-phase stoichiometric Ni₃FeN powder was synthesized by hydrothermal precipitation of the mixed metal hydroxide and then by ammonolysis reaction. Phase purity and crystallinity were ensured by XRD and EDS. Additionally, particle size and morphology were examined with SEM. Finally, with LSV measurements for OER performance, overpotential at 10 mV/cm² and Tafel Slope were found to be 359 mV and 127.8 mV/dec, respectively. To determine ECSA and EDLC, CV was recorded in the non-faradaic region at various scan rates ranging from 5 to 800 mV/s. The results of EDLC and ECSA were 595 μF/cm² and 2.92 cm², respectively. HER performance was found not to be significant. All electrochemical tests in the study were carried out in an alkaline electrolyte. The outcome of this study suggests that the Nickel-Iron Nitride compound is a potential candidate as an electrocatalyst for OER under alkaline conditions.

Keywords: Water Splitting, Nickel-Iron Nitride, Electrocatalysts, Oxygen Evolution Reaction.

1 Introduction

Water splitting is a key process for the transformation of electrical energy into chemical energy within a sustainability scope, and its significance advances gradually due to the increased energy demand of the world [1]. Inevitable depletion of fossil fuels in the future may be a reason for the increased attention on sustainable energy technology

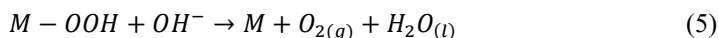
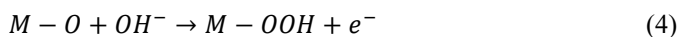
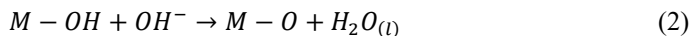
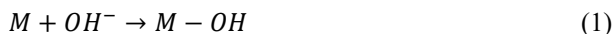
© The Author(s) 2026

R. Rzayev et al. (eds.), *Proceedings of the International Conference on Current Problems in Engineering and Applied Sciences (ICCPEAS 2025)*, Advances in Engineering Research 299,

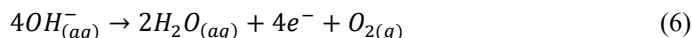
https://doi.org/10.2991/978-94-6239-668-5_27

from the scientific community and the authorities. Moreover, hydrogen, as a product of water splitting, is an abundant element in nature, and it provides three times higher energy than that of gasoline in the same quantity [2]. From this perspective, new developments in water splitting technologies become noteworthy.

Water splitting is based on two fundamental reactions, which are the hydrogen evolution reaction (HER) and the oxygen evolution reaction (OER). While the hydrogen evolution reaction requires the transfer of two electrons to proceed, the transfer of four electrons is needed for oxygen production [3]. In alkaline medium, the oxygen evolution mechanism follows the pathways below (M represents the catalyst surface) [4]:



The overall oxygen evolution reaction is,



The reaction can occur in two ways. One of them is step (1), step (2) and step (3). Also, the M-O intermediate, which emerges at step (2), can react with OH⁻, rather than other oxygen adsorbed on the surface, and forms M-OOH. Then, M-OOH reacts again with OH⁻ in electrolyte, and liquid water returns electrolyte while gaseous oxygen desorbs from surface.

However, OER proceeds in multiple steps, and single-electron transfer in each step makes it kinetically more sluggish [5]. Thus, catalytic materials play a vital role in achieving as low overpotential and high current density as possible when the OER process occurs. The well-known electrocatalysts for OER are IrO₂/RuO₂, and those for HER are Pt and its alloys, so they are also used as benchmark catalysts for the reactions, respectively [6]. However, their scarcity and high cost prevent their commercialization for industrial applications [7]. Therefore, the development of relatively abundant and low-cost catalyst materials has gained prominence, and transition metal nitrides are one of the groups of materials that have been extensively explored for OER.

Transition metal nitrides could be seen as a promising candidate for OER catalyst because they have unique properties such as their multi-valence states, special electronic structure, and physical properties [8]. For example, Nitrogen atoms introduced into transition metals cause d-band contraction and increase the density of d-electrons, which is similar to that of noble metals up to the Fermi Level [9]. In addition to the electronic structure advantages of transition metal nitrides, they show metallic conductivity and high corrosion resistance [10]. Thus, it can be utilized under harsh and realistic conditions [11].

In this study, we synthesized phase pure stoichiometric Ni_3FeN powders in order to measure the catalytic activity of it for the oxygen evolution reaction in a 1 M KOH electrolyte, which is saturated with nitrogen gas. The aim for the use of N_2 -saturated alkaline electrolyte is to obtain the true kinetic contribution of the electrocatalyst. Electrochemical measurements, cyclic voltammetry, and linear sweep voltammetry, were conducted to determine the catalytic activity of Ni_3FeN powder mixed with carbon black to facilitate easy electron transfer during the reaction proceeds.

2 Experimental Procedure

2.1 Synthesis and Characterization of Ni_3FeN

Synthesis. $\text{NiCl}_2 \cdot 6\text{H}_2\text{O}$ (Sigma-Aldrich, Reagent plus) and $\text{FeCl}_2 \cdot 6\text{H}_2\text{O}$ (Merck, ACS reagent, 99%) were used as precursor materials to synthesize nickel-iron nitride powder, and they were mixed with deionized water of 150 mL and 1000 mL, respectively. The moles of the precursors were determined according to the ratio of elements in the targeted compound. Also, 162.5 mmol of urea were mixed with 150 mL of deionized water. After complete dissolution of precursors, the nickel-containing solution was added to the iron-containing solution. Then, the urea solution was poured into the iron-nickel aqueous mixture slowly. After mixing all precursors, the solution was transferred into a stainless-steel reactor at 120 °C for 25 hours to synthesize Ni-Fe-hydroxide/oxy-hydroxide phases. When the synthesized hydroxide/oxy-hydroxide phases were cooled down to room temperature, they were centrifuged and washed with distilled water several times. Final washing was carried out with ethanol. Subsequently, it remained to be dried at 80 °C overnight; thereafter, they were ground in a mortar. The ammonolysis reaction occurred in a tube furnace under flowing NH_3 at 500 °C for 3 hours. The black powder obtained from the ammonolysis reaction was then ground in a mortar.

Characterization. The crystal structure of the synthesized powder was examined by X-Ray Diffractometer (XRD, Bruker D8 Advance, $\text{CuK}\alpha$). Scanning range and scan rate for X-Ray diffraction were 20°-80° and 5°/min. Morphology investigation and compositional analysis (EDS analysis) of the synthesized sample were performed under scanning electron microscopy (FE-SEM, Nova NanoSEM 430).

2.2 Electrode Preparation, Cell Configuration, and Electrochemical Measurements

Electrode Preparation. 50 mg of active material and 10 mg of carbon black (Printex L6), as a conductive additive, were mixed with 8 mL of ultra-high pure water and 2 mL of isopropyl alcohol by ultrasonicator for 15 min in an ice bath. Subsequently, 200 μL of Nafion™ solution (5% in isopropyl alcohol) was added to it. Then, it was sonicated once more for 15 min to properly disperse the binder into the mixture, which was now called ink. Afterwards, a mirror-finished glassy carbon rotating disc electrode was coated by 10 μL of prepared ink by drop casting, and it was dried at ambient conditions.

Cell Configuration and Electrochemical Measurements. The electrochemical cell consisted of three electrodes and an electrolyte. The working electrode was a rotating disc electrode coated with active material; a platinum electrode was used as a counter electrode, and a reversible hydrogen electrode (BioLogic, HydroFlex®) was the 1. a. 1. reference electrode in the cell configuration. Also, the alkaline electrolyte was 1.0 M of KOH (Merck, KOH > 85%, pellets) solution with a pH of 14.04

Before cyclic voltammetry (CV) and linear sweep voltammetry (LSV), N₂ gas was passed through the electrolyte at a flow rate of 1.5 L/min for 20 min. The reason for the preference of nitrogen gas was to understand the true kinetic evaluation of the catalyst. Also, to make the surface ready for electron transfer, conditioning CV was applied around 1.23 V±0.15 V (for OER) at 300 mV/s for 50 cycles while gas was bubbled into the solution, and the working electrode was not rotating. Then, the electrolyte was blanketed with N₂ gas during LSV. For OER, LSV was applied from 1.2 V to 1.6 V at a 5 mV/s sweep rate while the working electrode was rotating at 1600 rpm. To determine the electrochemically active surface area (ECSA) and electrochemically double-layer capacitance (EDLC), cyclic voltammograms were obtained at various scan rates (5, 10, 25, 50, 100, 200, 400, 800 mV/s) in the non-faradaic region (0.9-1.1 V) while nitrogen gas was used to blanket the electrolyte surface. The working electrode was not rotating during the CV measurements.

3 Results and Discussion

3.1 Characterization of the Synthesized Ni₃FeN Compound

The aim of synthesizing phase-pure Ni₃FeN was accomplished via hydrothermal precipitation, confirmed by XRD results (Fig. 2). The most intense and detectable peaks match the theoretical peaks. Thus, according to the peak positions taken from the ICDD database [12], a phase-pure nickel-iron nitride compound was obtained from the synthesis. On the other hand, weak 2 peaks around 54 and 60 degrees could be obscured by background noise. Moreover, EDS results support the deduction from XRD, indicating reasonably low impurity in the sample.

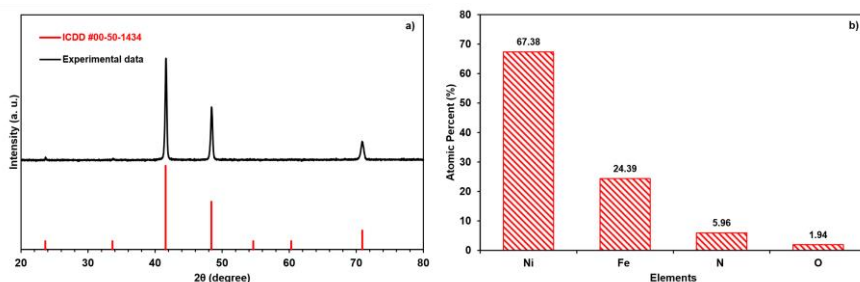


Fig. 1. a) XRD result of the synthesized Ni₃FeN (black), red lines indicate the theoretical peak positions according to ICDD database (ICDD card no. 00-050-1434) b) EDS result of Ni₃FeN.

As mentioned above, the synthesized powder was examined under SEM to understand the morphology and obtain a clue about the size of the particles. SEM images at different magnifications can be seen in Figure 3. The morphology of the sample can be described as the fact that irregularly shaped particles were interconnected with each other and formed a sponge-like network, which creates voids and openings. These features may increase the surface area. Furthermore, the size of some particles measured from SEM images provides a hint about the particle size, which supports the irregularity of the particles, ranging from 190.7 nm to as high as 593.0 nm.

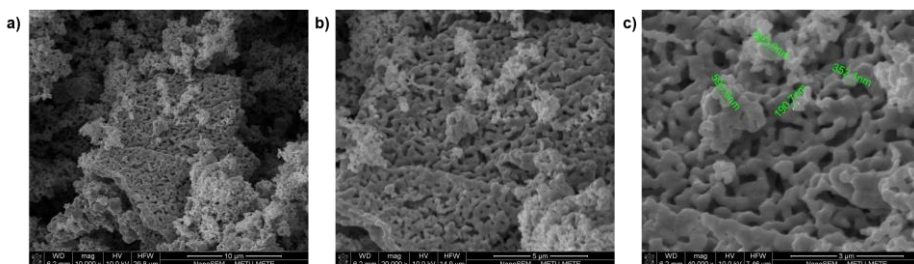


Fig. 2. SEM images of Ni₃FeN powders; a) 10 000x magnification, b) 20 000x magnification, c) 40 000x magnification with the particle size measured by using the scalebar.

3.2 Electrocatalytic Performance

Electrochemical double-layer capacitance and electrochemically active surface area of the Ni₃FeN/C were determined by carrying out cyclic voltammetry at various scan rates (Fig. 3a). The specific electrochemical double-layer capacitance (EDLC) of Ni₃FeN/C was found to be 595 $\mu\text{F}/\text{cm}^2$ from the slope of capacitive current density with respect to scan rate obtained via CV curves. Also, the roughness factor is 14.8. It was calculated simply by dividing the specific double-layer capacitance by the specific capacitance of an atomically flat and smooth surface (40 $\mu\text{F}/\text{cm}^2$ in 1 M KOH). Dividing the roughness factor by the geometric surface area of the electrode gives the electrochemically active surface area, which is 2.92 cm^2 .

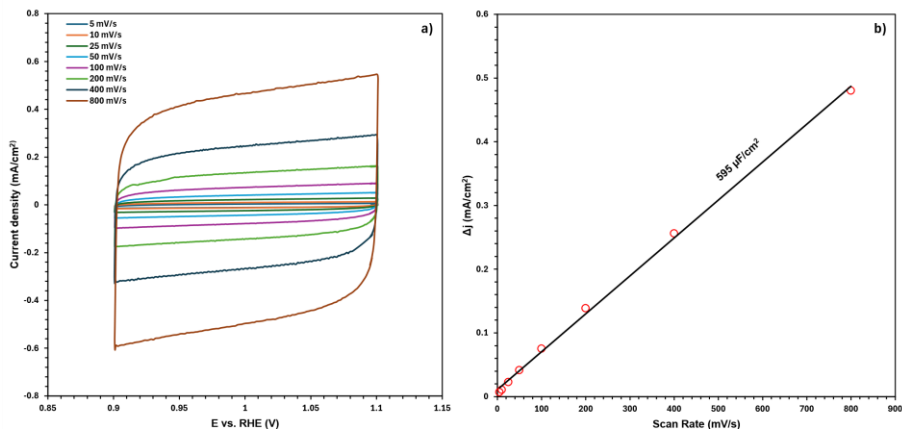


Fig. 3. a) cyclic voltammetry curves for $\text{Ni}_3\text{FeN/C}$ at various scan rates, b) capacitive current density change of $\text{Ni}_3\text{FeN/C}$ during CV with respect to scan rates; black line shows linear regression of data.

The linear sweep voltammetry (LSV) curve of the synthesized $\text{Ni}_3\text{FeN/C}$ compound and its Tafel slope is given in Figure 5. The overpotential at 10 mA/cm^2 current density is found to be 359 mV . According to the study of Putra et. al., commercially used IrO_2/C in N_2 -saturated 1 M KOH electrolyte shows 379 mV overpotential at 1 mA/cm^2 onset current density [13]. Furthermore, the same study states that the Tafel slope of IrO_2/C under the same conditions (in N_2 -saturated 1 M KOH) is 189 mV/dec [13]; on the other hand, $\text{Ni}_3\text{FeN/C}$ shows 127.8 mV/dec , which is lower than IrO_2/C . Therefore, $\text{Ni}_3\text{FeN/C}$ surpasses the commercial IrO_2 electrocatalyst for OER.

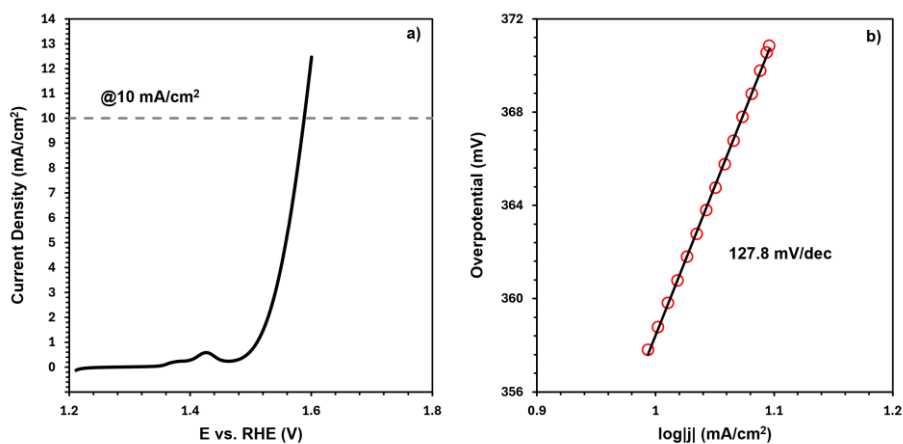


Fig. 4. a) Linear sweep voltammogram and b) Tafel slope of synthesized $\text{Ni}_3\text{FeN/C}$.

There is also an oxidation peak around 1.45 V in the LSV curve of Ni₃FeN/C. The study of Yu et. al., assigned the peak as oxidation of Ni⁺² to Ni⁺³ [14]. Thus, the oxidation peak shown around 1.45 V in Figure 5a is thought to be an Ni⁺²/Ni⁺³ oxidation.

4 Conclusion

Due to the increasing attention to green energy around the world, the importance of a new noble element-free electrocatalyst becomes emergent gradually. Therefore, a nickel-iron nitride compound was developed and characterized in terms of catalytic properties in this study. When developed Ni₃FeN/C compound was electrochemically tested, it was found that it exhibits remarkable electrocatalytic behavior, such as a relatively low overpotential at 10 mA/cm² onset potential, which is 359 mV in 1 M KOH electrolyte saturated with N₂. Also, the Tafel slope of Ni₃FeN/C was found to be 127.8 mV/dec. Moreover, the electrochemically active surface area (ECSA) was 2.92 cm² as well as the fact that the roughness factor was 14.8. When it is compared to commercial IrO₂/C from the point of catalytic activity, Ni₃FeN/C can be an encouraging candidate for a noble-element-free catalyst for oxygen evolution reaction.

Acknowledgments. The authors declare that this work received no specific funding and no external support.

Disclosure of Interests. There are no conflicts to declare.

References

1. S. Chu and A. Majumdar, "Opportunities and challenges for a sustainable energy future," *Nature*, vol. 488, no. 7411, pp. 294–303, 2012, doi: 10.1038/nature11475.
2. P. Chen, J. Ye, H. Wang, L. Ouyang, and M. Zhu, "Recent progress of transition metal carbides/nitrides for electrocatalytic water splitting," *J Alloys Compd*, vol. 883, p. 160833, 2021, doi: <https://doi.org/10.1016/j.jallcom.2021.160833>.
3. Y. Jiao, Y. Zheng, M. Jaroniec, and S. Z. Qiao, "Design of electrocatalysts for oxygen- and hydrogen-involving energy conversion reactions," *Chem Soc Rev*, vol. 44, no. 8, pp. 2060–2086, 2015, doi: 10.1039/C4CS00470A.
4. A. K. Samantara and S. Ratha, "Mechanism and Key Parameters for Catalyst Evaluation," in *Metal Oxides/Chalcogenides and Composites: Emerging Materials for Electrochemical Water Splitting*, A. K. Samantara and S. Ratha, Eds., Cham: Springer International Publishing, 2019, pp. 11–29. doi: 10.1007/978-3-030-24861-1_3.
5. X. Peng, C. Pi, X. Zhang, S. Li, K. Huo, and P. K. Chu, "Recent progress of transition metal nitrides for efficient electrocatalytic water splitting," *Sustain Energy Fuels*, vol. 3, no. 2, pp. 366–381, 2019, doi: 10.1039/C8SE00525G.

6. T. Y. Ma, S. Dai, M. Jaroniec, and S. Z. Qiao, "Graphitic Carbon Nitride Nanosheet–Carbon Nanotube Three-Dimensional Porous Composites as High-Performance Oxygen Evolution Electrocatalysts," *Angewandte Chemie International Edition*, vol. 53, no. 28, pp. 7281–7285, Jul. 2014, doi: <https://doi.org/10.1002/anie.201403946>.
7. Q. Shi, C. Zhu, D. Du, and Y. Lin, "Robust noble metal-based electrocatalysts for oxygen evolution reaction," *Chem Soc Rev*, vol. 48, no. 12, pp. 3181–3192, 2019, doi: 10.1039/C8CS00671G.
8. Y. Zhong, X. Xia, F. Shi, J. Zhan, J. Tu, and H. J. Fan, "Transition Metal Carbides and Nitrides in Energy Storage and Conversion," *Advanced Science*, vol. 3, no. 5, p. 1500286, May 2016, doi: <https://doi.org/10.1002/advs.201500286>.
9. D. J. Ham and J. S. Lee, "Transition Metal Carbides and Nitrides as Electrode Materials for Low Temperature Fuel Cells," *Energies (Basel)*, vol. 2, no. 4, pp. 873–899, 2009, doi: 10.3390/en20400873.
10. S. Dong, X. Chen, X. Zhang, and G. Cui, "Nanostructured transition metal nitrides for energy storage and fuel cells," *Coord Chem Rev*, vol. 257, no. 13, pp. 1946–1956, 2013, doi: <https://doi.org/10.1016/j.ccr.2012.12.012>.
11. A. K. Tareen, G. S. Priyanga, K. Khan, E. Pervaiz, T. Thomas, and M. Yang, "Nickel-Based Transition Metal Nitride Electrocatalysts for the Oxygen Evolution Reaction," *ChemSusChem*, vol. 12, no. 17, pp. 3941–3954, Sep. 2019, doi: <https://doi.org/10.1002/cssc.201900553>.
12. X. G. Diao, F. S. Li, Z. J. Zhao, and S. Q. Zhou, "Preparation and characterization of γ' -Ni₃FeN," *J Mater Sci Lett*, vol. 15, no. 18, pp. 1590–1591, 1996, doi: 10.1007/BF00278098.
13. R. P. Putra, H. Horino, and I. I. Rzeznicka, "An Efficient Electrocatalyst for Oxygen Evolution Reaction in Alkaline Solutions Derived from a Copper Chelate Polymer via In Situ Electrochemical Transformation," *Catalysts*, vol. 10, no. 2, 2020, doi: 10.3390/catal10020233.
14. L. Yu *et al.*, "Non-noble metal-nitride based electrocatalysts for high-performance alkaline seawater electrolysis," *Nat Commun*, vol. 10, no. 1, p. 5106, 2019, doi: 10.1038/s41467-019-13092-7.

Open Access This chapter is licensed under the terms of the Creative Commons Attribution-NonCommercial 4.0 International License (<http://creativecommons.org/licenses/by-nc/4.0/>), which permits any noncommercial use, sharing, adaptation, distribution and reproduction in any medium or format, as long as you give appropriate credit to the original author(s) and the source, provide a link to the Creative Commons license and indicate if changes were made.

The images or other third party material in this chapter are included in the chapter's Creative Commons license, unless indicated otherwise in a credit line to the material. If material is not included in the chapter's Creative Commons license and your intended use is not permitted by statutory regulation or exceeds the permitted use, you will need to obtain permission directly from the copyright holder.

